Materials Chemistry and Physics 287 (2022) 126343

Contents lists available at ScienceDirect

Materials Chemistry and Physics

journal homepage: www.elsevier.com/locate/matchemphys

Ti–Ta dental alloys and a way to improve gingival aesthethic in contact with the implant

Iosif Hulka [a], Nestor R. Florido-Suarez [a], Julia C. Mirza-Rosca [a,*], Adriana Saceleanu [b]

[a] Las Palmas de Gran Canaria University, Department of Mechanical Engineering, Tafira, 35017, Spain
[b] Lucian Blaga University of Sibiu, Medicine Faculty, 550024, Sibiu, Romania

HIGHLIGHTS

- New Ti-xTa dental alloys were fabricated using the levitation fusion technique.
- Varying the potential, different colors might be obtained through passivation on the surface of the Ti-xTa samples.
- The hardness of the oxide layer rich the maximum value at 25%Ta.
- Using a potential of 70 V a reddish oxide color was obtained which might have optimal applications in dentistry.

GRAPHICAL ABSTRACT

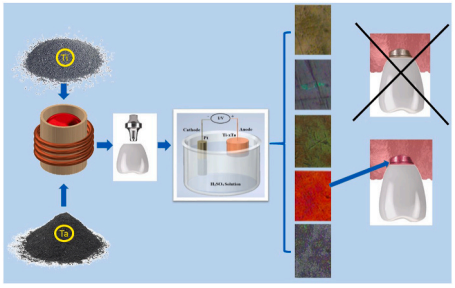

ARTICLE INFO

Keywords:
Ti-Ta
Dental alloys
Oxide growth
Passivation
Mechanical properties

ABSTRACT

The development of Ti-based alloys with improved properties for medical applications is a challenge nowadays in the field of materials engineering. In this study, the color of oxide layers developed by anodic oxidation in H_2SO_4 solution on Ti–Ta alloys was studied and the alteration in microhardness was evaluated. The alloys were manufactured by levitation fusion technique using Ti as base material and Ta was added in 5, 15, 25, and 30 wt%. After the alloys were passivated, changes of oxide color function of applied potential, the growth of oxide mass and the microhardness were investigated. The studies showed that the oxide mass increases with the potential and the hardness values vary as a function of Ta addition. The microhardness results showed that the oxide layer developed after passivation on the surface of Ti–25Ta alloy exhibited higher hardness values and a denser oxide layer as compared to the Ti–5Ta, Ti–15Ta, and Ti–30Ta alloys. Using a potential of 70 V a redish oxide color was obtained which might have optimal aplications in dentistry due to its aesthetics and mechanical properties.

1. Introduction

Ti and its alloys are currently widely used in medicine for the manufacture of dental and orthopedic implants. They have excellent corrosion resistance, good mechanical properties and high biocompatibility [1]. Among the qualities of Ti, an important one is the instant development of an oxide layer on its surface which enhances the corrosion resistance of the material in oxidizing acids and neutral media. However, it has a drawback, a lower resistance in reducing acids [2,3].

To enhance its properties, Al and V were added and for a very long time, the composition Ti–6Al–4V was used to manufacture medical implants [1]. Thus, lately, it was discovered that the composition has

* Corresponding author.
E-mail address: julia.mirza@ulpgc.es (J.C. Mirza-Rosca).

https://doi.org/10.1016/j.matchemphys.2022.126343
Received 30 March 2022; Received in revised form 26 May 2022; Accepted 31 May 2022
Available online 1 June 2022

Table 1
Chemical composition of row materials [%].

Row material	Fe	N2	O2	H2	C	Ti	Si	Mo	W	Ni	Nb	Ta
Ti	0.20	0.03	0.18	0.015	0.08	balance	-	-	-	-	-	-
Ta	0.01	0.01	0.03	0.0015	0.01	0.01	0.05	0.02	0.01	0.01	0.2	balance

Table 2
Mass composition of newly manufactured alloys.

Element	Alloy 1 (%)	Alloy 2 (%)	Alloy 3 (%)	Alloy 4 (%)
Ti	95	85	75	70
Ta	5	15	25	30

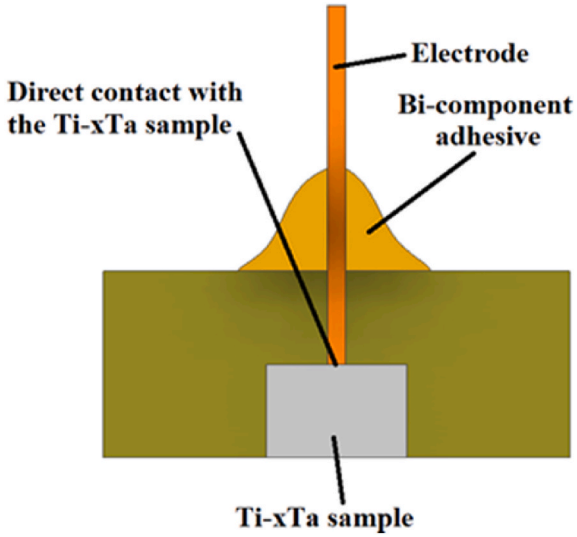

Fig. 1. Schematic representation of a Ti-xTa sample mounted in resin.

significant toxicity on the human body leading to health problems due to the release of V and Al ions [4,5]. In order to overcome these health problems of the human body, different Ti-based alloys were manufactured with non-toxic β-Ti type elements like Nb, Zr, Ta, etc. [6–8]. Besides the non-toxicity, a biocompatible alloy needs to have high corrosion resistance, high strength, a low Young's modulus similar to that of the bone and a certain roughness on the surface to ensure good osseointegration [9].

Among the non-toxic elements used to manufacture biocompatible alloys, Ta has an extraordinary resistance to corrosion caused by the formation of a Ta_2O_5 protective film [10]. Ti–Ta alloys are materials with improved properties compared to Ti and Ta when used individually. There are several manufacturing methods of Ta–Ti alloys in order to produce biocompatible materials. Thus, Hamzah et al. reported Ti–Ta alloys manufactured via casting, spark plasma sintering, compaction and microwave sintering [11]. Pedro P. Socorro-Perdomo et al. produced Ti–Ta alloys by levitation fusion in a high-frequency induction furnace [9]. Patricio et al. manufactured Ti–Ta alloys by arc melting method in an atmosphere of argon with tungsten electrode in a copper crucible refrigerated by water [12]. Disregarding the manufacturing method, new Ti–Ta alloys have been developed and are expected to become promising candidates for dental applications [13].

To obtain the growth of the oxide layer on Ti–Ta surface, the alloy is passivated at different voltages in liquid media. When the alloy is passivated in an electrolyte within an electrochemical cell and a counter electrode is used, the transport of ions is responsible for the oxide layer growth which depends on the potential used in the process [14]. By anodic oxidation, different colors can be obtained by controlling the amount of oxides on the surface which interacts differently with the light. Studies have shown that the anodized Ti develops oxide layers which can improve gingival aesthetics by masking the gray color of Ti [15]. Esthetically, one of the shortcomings of titanium is its grayish aspect through thin mucosa, which can result in a reduction of patient compliance with implant-supported replacements [16–18]. Charrière et al. reported that an increase of the Ti oxide layer enhances the surface hardness and corrosion resistance [19].

However, only of few investigations of the oxide layer developed on the surface of Ti–Ta alloys obtained through passivation were found in the literature. Most of the research is focused on microstructural characterization [4], biocompatibility [20] and corrosion behavior [21] of the bulk material. Thus, the purpose of the present study was to evaluate the influence of voltage on the oxide color and oxide mass growth developed on the surface of Ti-xTa (x = 5, 15, 25, and 30 wt%) alloys passivated in H_2SO_4 solution. The mechanical properties in terms of microhardness were studied as well. There is no data available about this particular oxide developed at different passivation voltages on the surface of Ti–Ta alloys manufactured by the levitation fusion technique.

2. Materials and methods

2.1. Ti–Ta alloys preparation

According to the manufacturer, the primary materials employed in the present study are commercially available and their chemical composition is presented in Table 1.

The studied Ti–Ta alloys were manufactured by the levitation fusion technique using an induced furnace operated with a cold copper crucible at 2000 °C at 10^{-4} mbar primary vacuum, and a 3×10^{-8} mbar secondary vacuum. Argon was used to protect the samples against oxidation. The new alloys were produced under ingot shape with a 20 mm diameter and a 30 mm length, using the mass composition presented in Table 2. To avoid segregation, homogenization heat treatment was performed in a furnace using the following heat treatment conditions: (a) homogenization temperature 1000 °C, (b) heating rate, 5 °C/min and (c) natural cooling. After homogenization treatment, EDS measurements were carried out with an environmental scanning electron microscope with an energy dispersive X-ray electron sample analyzer and it was observed that there are no impurities and that titanium and tantalum were the only identified elements in a homogeneous and segregation-free metallic mass [9].

To analyze the samples, the ingots were cut using an automatic linear saw (IsoMet 4000 Precision Saw, Buehler) that allows precise cutting of delicate samples without deformation. Afterward, the 2 mm high specimens were mounted in acrylic resin to protect the edges of the samples during the grinding process. A copper wire was attached to the samples as presented in Fig. 1 to ensure the electrical contact between the working electrode and the power source.

Grinding was performed on a Struers TegraPol-11 polishing machine using SiC papers up to 2500 grit size, followed by polishing using 0.1 μm alpha-alumina suspension. The samples were ultrasonically cleaned and then rinsed with distilled water and ethanol to remove the suspension from the surface.

2.2. Anodic oxidation and color characterization

The four specimens underwent a surface treatment with sulfuric acid, which favored the creation of an oxide film on the surface of the samples. For this, the specimens were immersed in a solution of H_2SO_4 3 M

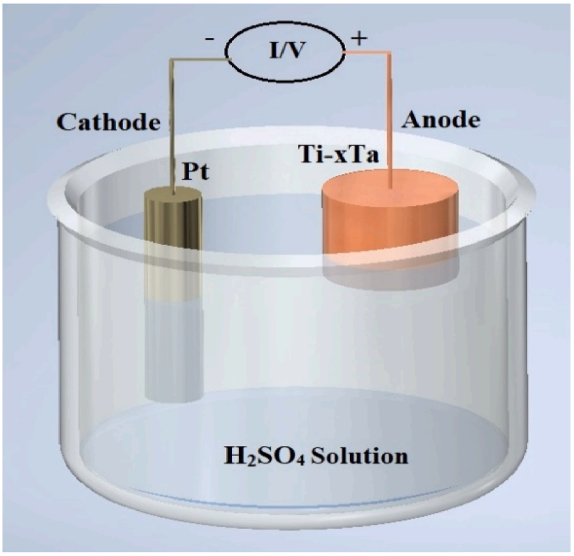

Fig. 2. Schematic reprezentation of the electrochemical anodization cell used to fabricate oxide layers on Ti-xTa samples. The Ti-xTa samples were used as anodes and Platinum was used as cathode in a H_2SO_4 electrolyte solution.

for 60 s. The experimental setup consisted of a Hi-Tron power source connected to a multimeter and an electrochemical cell. Four sources of voltage, one at 30 Vcc, the other 24 Vcc and two of 50 Vcc have been selected for this experiment. Therefore it was decided to connect two sources in series while the other two in parallel in order to perform the tests. To ensure that the potential was constant all times, the voltmeter was connected between the working and reference electrode while a multimeter was connected to one of the voltage sources and it was used as an amperemeter. The electrochemical anodization cell is presented in Fig. 2.

After 1 min of testing, the new oxide layer formed on the surface of the alloys was analyzed under the microscope. This procedure was repeated every 10 V up to 100 V. Thus, these values were chosen to observe how the potential affects the color of the samples and to determine the current intensity (mA). The current intensity is useful for determining the mass of oxide formed on the surface of the samples by using the formula of Faraday's Laws.

The influence of different voltages on the anodized samples was investigated using an Olympus metallographic microscope, model PME 3-ADL equipped with an ELMO color CCD TV Camera, model TPC5502EX.

2.3. *Phase structure*

The phase structure was identified by X-ray diffraction (XRD) on an Empyrean diffractometer (Malvern-Panalytical) with Cu Kα radiation at room temperature. The measurements were performed at an angle of 2θ

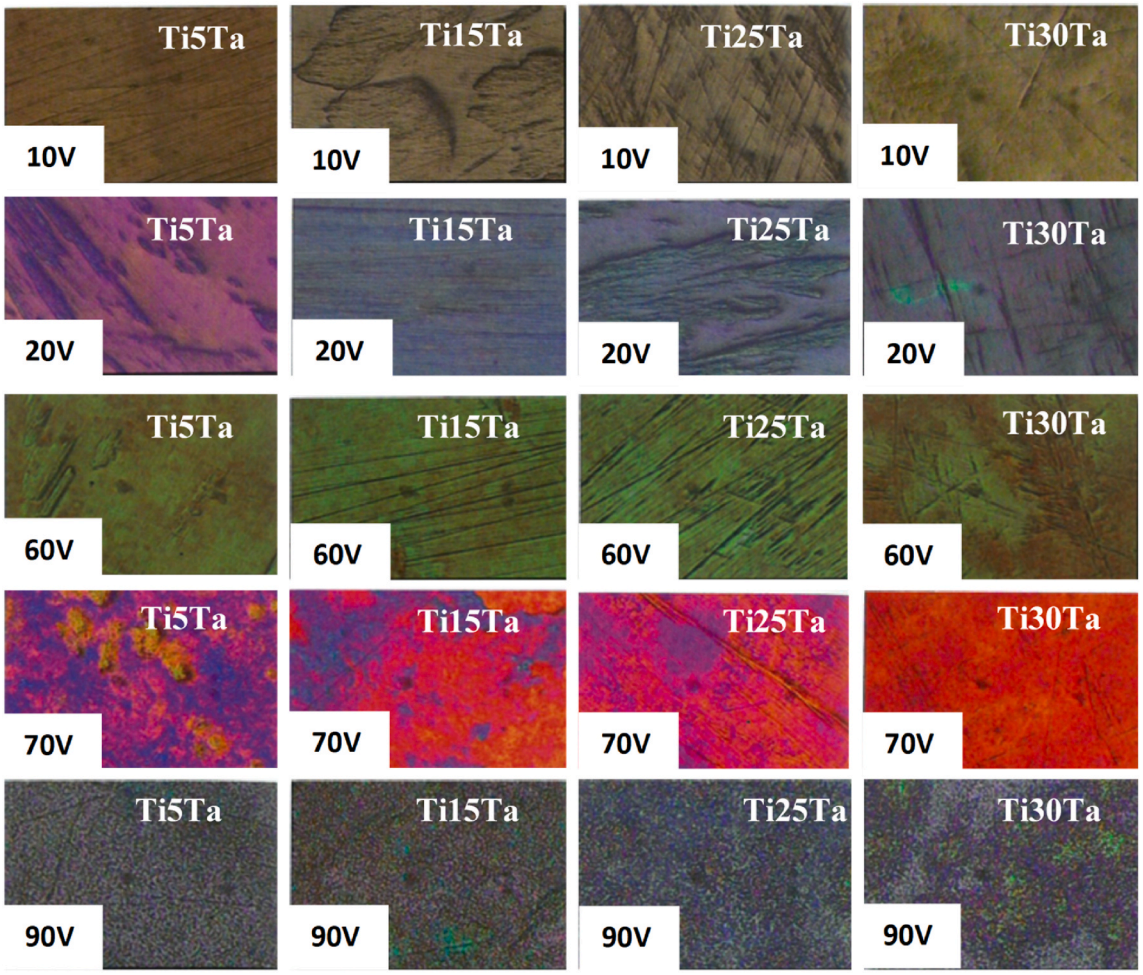

Fig. 3. Color change of samples after passivation at different voltages. (For interpretation of the references to color in this figure legend, the reader is referred to the Web version of this article.)

Table 3
HTML color names and hex codes of the oxide layer formed on the Ti–Ta alloys at different voltages.

Voltage [V]	Ti5Ta		Ti15Ta		Ti25Ta		Ti30Ta	
	Hex code	Name	Hex code	Name	Hex code	Name	Hex code	Name
10	#80461 B	Russet	#988558	DarkTan	#988558	DarkTan	#C2B80	DarkTan
20	#DA70D6	Orchid	#B0C4DE	LightSteelBlue	#B0C4DE	LightSteelBlue	#B0C4DE	LightSteelBlue
30	#7393B3	Blue gray	#7393B3	Blue gray	#7393B3	Blue gray	#7393B3	Blue gray
40	#6082B2	Glaucous	#6082B2	Glaucous	#6082B2	Glaucous	#6082B2	Glaucous
50	#7393B3	Blue gray	#7393B3	Blue gray	#7393B3	Blue gray	#7393B3	Blue gray
60	#808000	OliveDrab	#808000	OliveDrab	#808000	OliveDrab	#808000	OliveDrab
70	#80080	Purple	#FA5F55	Sunset orange	#FA5F55	Sunset orange	#FF4433	Red orange
80	#40B5AD	Verdigris	#40B5AD	Verdigris	#40B5AD	Verdigris	#40B5AD	Verdigris
90	#71797E	Steel gray	#71797E	Steel gray	#71797E	Steel gray	#71797E	Steel gray
100	#A9A9A9	Dark gray	#A9A9A9	Dark gray	#A9A9A9	Dark gray	#A9A9A9	Dark gray

Table 4
Current density [mA/cm^2].

Voltage [V]	Ti5Ta	Ti15Ta	Ti25Ta	Ti30Ta
10	0,22	0,33	0,36	0,38
20	0,63	0,85	1,2	1,32
30	1,2	1,4	1,9	2,01
40	2,3	2,4	2,47	2,52
50	3	3,05	3,44	3,61
60	3,88	4	4,05	4,03
70	4,6	5,1	5,21	5,33
80	5,2	5,94	6,7	6,98
90	5,5	6,64	7,45	7,67
100	5,8	7,5	8,6	8,9

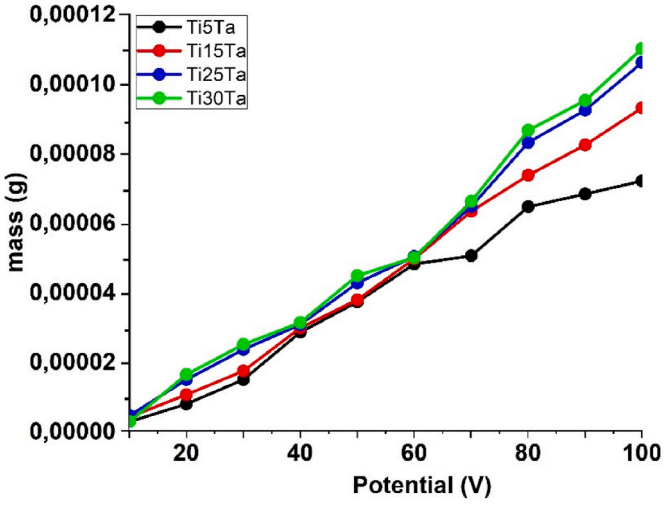

Fig. 4. Changes in the mass of oxide layers formed on the surface of the samples passivated for 60 s in H_2SO_4 solution *XRD*.

in the range of 30–65° with a step size of 0.04° at a power of 45 kV.

2.4. Microhardness and indentation depth

The microhardness of the Ti–Ta alloys was measured by a BUEHLER Microhardness Tester, using 5, 10, 20 50 and 100 mNloads with a 15 s holding time. For each sample, 10 points were tested on the surface of the oxide layer to confirm the reproducibility and reliability of the results.

The depth of indentation (δ) left on the surface by the pyramidal indenter during hardness measurements can be determined from the relationship between the depth of the footprint and the diagonal of the indentation in relation to the applied load (F) and the hardness value (HV). Taking into account that Vickers indenter tip is a four-sided pyramid with 136° as the included angle between plane faces of the pyramid, thus, the depth of indentation can be determined by using the following equation obtained from general Vickers equation:

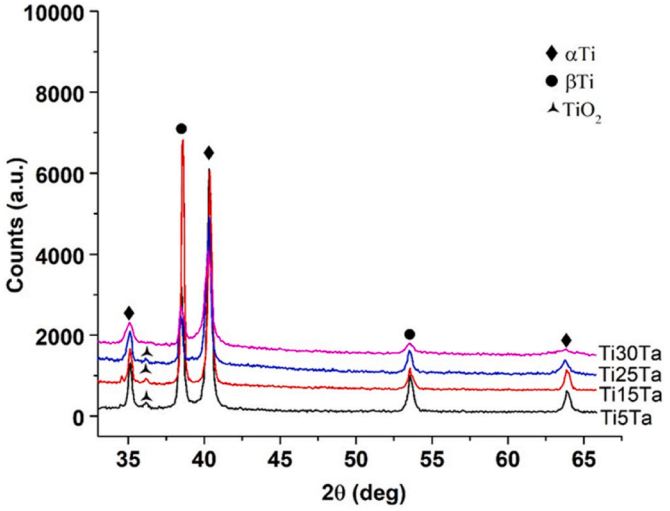

Fig. 5. XRD spectra for TixTa alloys.

$$\delta = \sqrt{\frac{1.854 \cdot F}{49 \cdot HV}} \quad (1)$$

where: δ - the depth of indentation, F - applied load, HV - hardness value.

3. Results and discussions

3.1. Color characterization

Fig. 3 shows the obtained colors after passivation at different voltages in H_2SO_4 3 M solution. Only representative images are presented, obtained at 10, 20, 60, 70, and 90 V. The colors formed on the Ti–Ta alloys' surface after passivation are commonly referred to as interference colors. It is known that there is no pigment associated with these changes [21] and that the interferences of waves within the oxide layer are the main cause of color change when Ti alloys are passivated in the H_2SO_4 solution [22].

It can be observed that not all colors correspond to a general color that was characterized, i.e., when we speak of green color it is not a pure one. Among the samples passivated with the same voltage, there are other shades of the same color. In fact, the image collected by the microscope usually has a margin of error with respect to the hue of the color. This "muted tonality" or "low contrast" effect is due to the camera attached to the microscope. Thus, there are differences when one visualizes the specimens with the naked eye and when viewed through the lenses of the microscope. For this reason, the images passivated at 100 V,

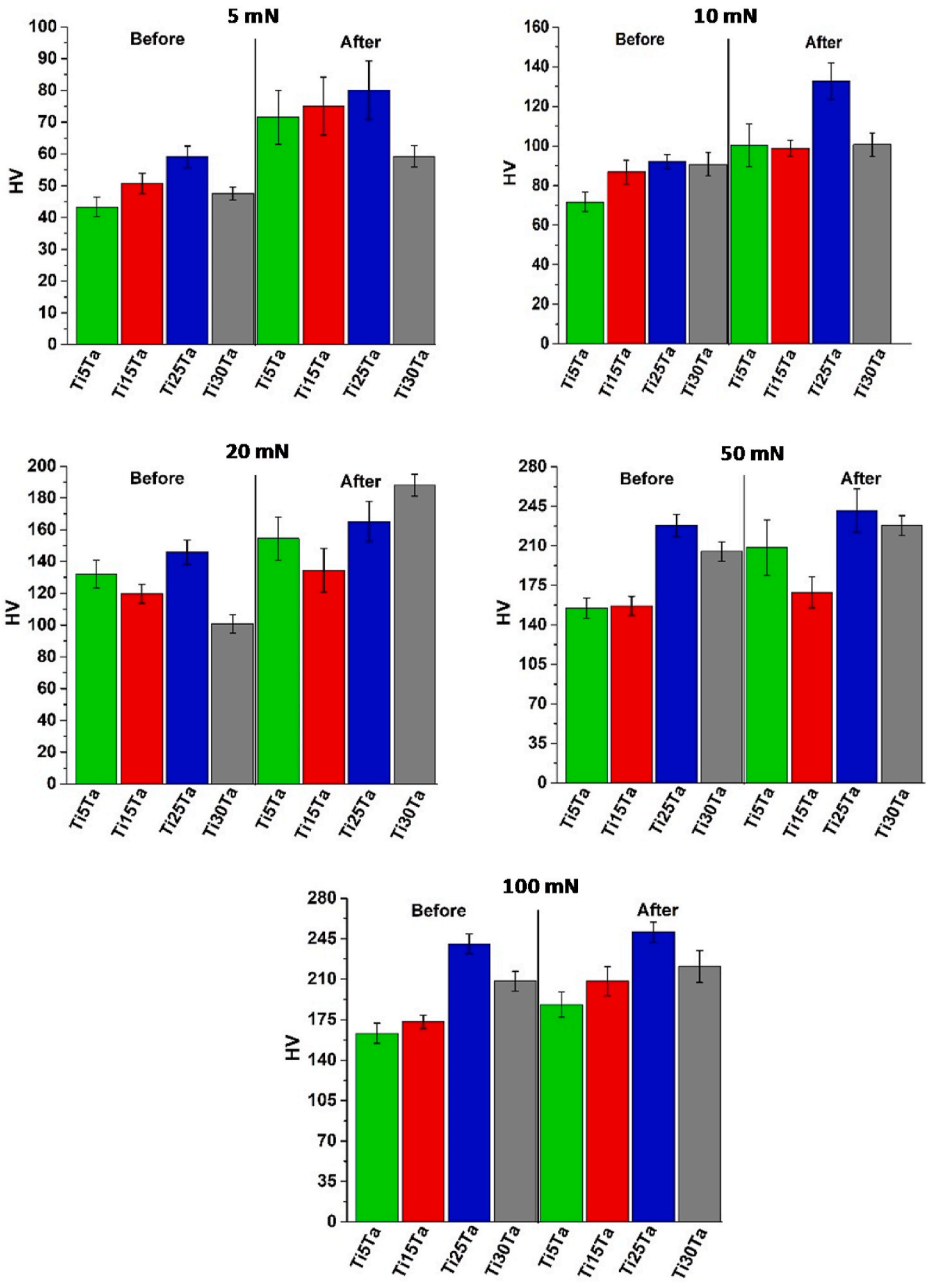

Fig. 6. Hardness measurements on Ti-xTa samples under different loads before and after anodizing.

are presented at a magnification of 600× because the best resolution was obtained with this setup.

The color of the layers obtained by anodizing is attributed to light interferences phenomena within the oxide surface film and is mainly determined by its thickness [22]. Other factors influencing the characteristics of the oxide layer resulting from the anodizing process are the working parameters of the applied process: anodizing voltage and current density of anodization, duration of the process, characteristics of electrolyte (composition, pH, concentration, temperature, agitation) and also chemical composition and surface finishing of the samples [23].

Under anodic polarization, a layer of TiO is formed at the beginning:

$$Ti + H_2O = TiO + 2H^+ + 2e^- \quad (2)$$

As the potential is increasing, this is transformed to Ti_2O_3:

$$2TiO + H_2O = Ti_2O_3 + 2H^+ + 2e^- \quad (3)$$

And finally to TiO_2:

$$3Ti_2O_3 + H_2O = 2Ti_3O_5 + 2H^+ + 2e^- \quad (4)$$

$$Ti_2O_3 + H_2O = 2TiO_2 + 2H^+ + 2e^- \quad (5)$$

$$Ti_3O_5 + H_2O = 3TiO_2 + 2H^+ + 2e^- \quad (6)$$

So, the global reaction is:

$$Ti + 2H_2O \rightarrow TiO_2 + 4H^+ + 4e^- \quad (7)$$

For Ti, the Porbaix diagram of Ti–H_2O [24] shows that the significant reduction in passive film strength at potentials near 1 V can be explained by the growth of $TiO_3{\cdot}H_2O$ on the surface of the alloys.

The Pourbaix Ta–H_2O diagram [24] indicates that the high resistance of tantalum is due to the formation of a protective layer of tantalum pentoxide (Ta_2O_5). Tantalum, under anodic polarization, has the tendency to be coated with this Ta_2O_5 film which is compact, continuous, etc., and the reaction that occurs is:

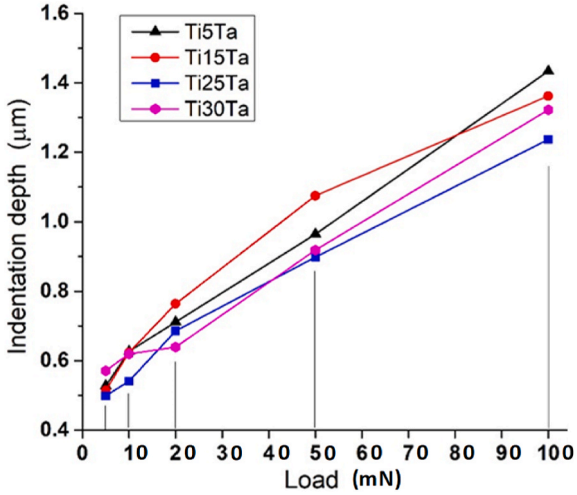

Fig. 7. Indentation depth after anodization.

$$2Ta + 5H_2O \rightarrow Ta_2O_5 + 10H^+ + 10e^- \quad (8)$$

We have considered only the total equation of the formation of Ta_2O_5 because of the great protective power of the layer of oxide which screens the metal from contact with the solution, at least in the absence of complexing substances in the physiological fluids [24].

Tantalum pentoxide can be found in the hydrated form; it has a different amount of water of crystallization and is assigned the formulation $Ta_2O_5{\cdot}H_2O$ or $HTaO_3$.

Table 3 presents the changes in the interference color of the oxide layer formed on the Ti–Ta alloys at a potential from 10 V to 100 V. The samples were characterized by using the HTML color names and hex codes to detect the correct colors and their differences. One can notice that the colors change from Dark Tan to Light Steel Blue and then to Blue Gray and so on, until a Dark Gray color is obtained. The dark gray color is achieved at a potential of 100 V which indicates that the oxide layer is thick enough and does not reflect anymore the light. Thus, the coloration of the oxide layer obtained by using different voltage values can be indicative of the thickness of the oxide layer [25]. This is very important taking into account that the titanium and tantalum oxide layers are responsible for the biocompatibility and ability to osseointegrate [26–29].

3.2. Current density

The current density was measured in order to determine the mass of oxides formed on the surface of the samples. Thereby, the current density was measured at different passivation voltages and the results are presented in Table 4. From this table, one can notice that the current density is related to the passivation voltage, and it growths for each Ti–Ta composition as the voltage increases. It was noticed as well that the current density slightly increase with the amount of Ta added to the alloy. This might be attributed do to the fact that Ta is a better conductor of electricity and it can handle much more electric current compared to Ti.

3.3. The effect of passivation voltage on the oxide layers

Fig. 4 shows the changes in the mass of the oxide layer versus different voltages used in the experimental part of the present study. The mass of the oxide layer was calculated by using Faraday's Laws formula and it can be seen the mass of oxides was directly related to the passivation voltage. This is in accordance with the studies of Karambakhsh et al. [21]. Among the applied voltages, the lowest amount of oxide was obtained for the samples anodized at 5 V and the highest amount of oxide for the samples anodized at 100 V. The high reactivity of titanium and high affinity for oxygen causes the samples to be covered with a very thin oxide film in the passivation process. By adding tantalum in the alloy, two types of oxides are forming, TiO_2 and Ta_2O_5 respectively, as was presented by Mardare et al. [30]. The newly obtained passive layer provides enhanced corrosion resistance for the Ti–Ta alloys.

Fig. 5 presents the XRD spectra of the investigated alloys. The analysis confirms the presence of α phase with a hexagonal close-packed structure which is a supersaturated solid solution and a β phase with a body-centered cubic structure which are the main phases of the alloys. This is attributed to the substrate material which is α- β Ti alloy. The intensity of the α phase decreased with the increase of Ta content within the composition which is attributed to different volume fractions of the α phase. A minor phase of TiO_2 was identified as well within the samples with Ta concentration up to 25%. The phase was more intense in the Ti5Ta sample and its intensity decreased with the increase of Ta content. Thus, in the sample with 30% Ta it was not detected which might be attributed to the lower fraction of Ti compared to the other investigated samples. Ta_2O_5 was not detected which might be attributed to a weak signal but also to the fact that titanium is a passivity promoter and Ta is a dissolution moderator [31,32].

3.4. Microhardness measurements

Measuring the Vickers hardness of metallic materials require a high quality sample surface. The measurements have been made in accordance with ISO 14577–1:2015 Metallic materials — Instrumented indentation test for hardness and materials parameters — Part 1: Test method. For each sample, microhardness measurements were performedby a Vickers indenter under 0.5, 1, 2, 5, and 10 g loads. The mean value of microhardness was calculated as an average of 10 indentations made on the surface of the samples before and after anodizing and the results are presented in Fig. 6. The results show that all the anodized samples presented higher surface hardness compared to the non-treated samples, in line with other study [33] which reflects the effects of transition from the substrate's metallic bond to the oxide layer's covalent bond. It can be seen that the hardness values increase with the increase of applied load for each composition. These results are contradictory with the general microhardness rules where the microhardness depends on the indentation load. These phenomena usually

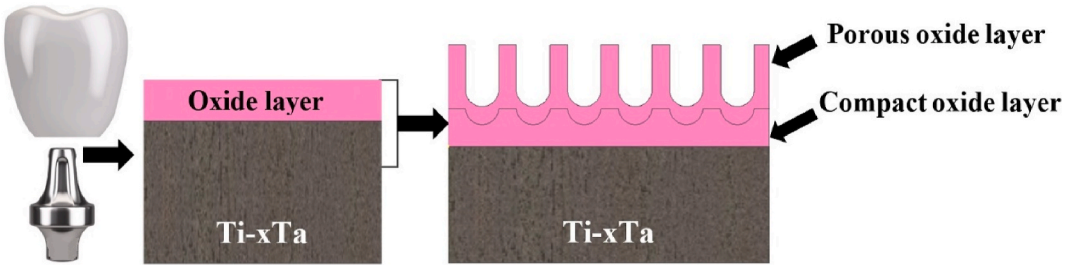

Fig. 8. Schematic representation of the oxide layers obtained after the electrochemical anodization process on the surface of Ti-xTa samples.

involve a decrease in the apparent microhardness while the applied testing load increase, thus with the increase of indentation size [34]. Jozef Petrík et al. found in their research that the microhardness increases with increasing load up to 30 g, a performance that is characteristic for a low load range [35] which is in accordance with our results.

It can be observed that with a load of 2 g the microhardness is increasing much (almost double comparing with 1 g load) and these results might be attributed as well to the top porous oxide layer obtained after passivation. The indentations with loads of 10 g shows that the microhardness of the oxide layer is higher than that of porous layer and even than that of bulk materials (136HV for Ti–5Ta, 144HV for Ti–15Ta, 202HV for Ti–25Ta and 180HV for Ti–30Ta, tests performed with a load of 2 N) and this can be explain by the existence of on inner oxide layer; this inner layer is dense and compact. By electrochemical impedance spectroscopy (EIS) we have concluded [9] that for a long immersion period in simulated body fluid, the passive film is thicker and develops this bi-layer structure: an outer porous layer and an inner compact layer.

Comparing the results presented in Fig. 6, one can see that in general, the hardness value increases with the addition of Ta, until the 25% percentage of tantalum is achieved. However, there are some exceptions. The sample with 15%Ta addition presents lower hardness values when tested under 2g and 5g load. The decline might be attributed to the lower relative density within the Ti–15%Ta alloy and the increase might be caused due to the solid solution reinforcement and grain fineness. Other studies also presented that the microhardness of Ti–Ta alloys fabricated through Selective Laser Melting (SLM) process decreased when 6 wt% of tantalum was added to the alloy and afterward it started to increase up to 25% wt. Ta [36].

In our study, when 30% of Ta was added, the hardness started to decrease under all the applied loads; it was also presented that the elastic modulus of Ti–Ta alloys decrease when the addition of Ta is more than 30% wt. Within the alloy [37]. It is well known that Ta is a β phase former in Ti-based alloys and that Ti-xTa alloys microstructure consists of a mixture mainly formed of α phase and β phase while α′ and α" are non-equilibrium martensite-type phases [38]. It was noticed that the intensity of the α'' phase decreased with the increase of Ta addition within the alloy, ascribed to the changes in the volume fraction of the α'' phase within the alloy [39] which has a significant influence on the mechanical properties. Thus, an increase of the β phase and the grain refinement does not always improve determinated mechanical properties of the alloy. In a similar way, this behavior could be overtaken by the passive layer developed on the surface of the tested samples. This might be attributed to the different transport numbers of Ta and Ti reported for thicker oxide layers developed on the surface of alloys [30].

In our study, the passivated oxide layer developed on Ti–25%Ta alloy proved to have the highest hardness value. Similar findings were presented by Pedro P. Socorro-Perdomo et al. [9] which showed that passive layers developed on these alloys have improved the mechanical behavior in terms of elastic modulus and enhanced corrosion resistance.

3.5. Indentation depth

The indentation depth results calculated after hardness measurements, using the formula presented at 2.3. Are presented in Fig. 7. It can be noticed when the load increases, the indentation depth also increase. When the applied load varied from 5 mN to 100 mN the indentation depth at least doubled for each composition. Analyzing the indentation depth for each composition one can notice that the differences slightly change, thus the Ti25Ta composition generally presents the lowest indentation depth indicating that the intender encountered a higher resistance during the test. This indicates that the oxide layer is more compact compared to the other oxide layers investigated in this study.

A significant influence on the hardness measurements, thus on the indentation depth is attributed to oxide structure developed on the surface of the samples. The oxide layer which forms on the surface is composed basically of two layers: a dense and compact layer deposited directly on the material and the second one developed on the compact layer presenting a more porous structure compared to the first one as it is presented in Fig. 8. The porous layer developed through passivation is of great importance since has an important part to play in the successful osseointegration due to the fact that the cells adhere well to the rough and porous substrates, demonstrating good spreading and proliferation behavior on the Ti-xTa alloys [33].

4. Conclusions

In the present study, the influence of the passivation voltage in H_2SO_4 solution on the development of oxide layers on new Ti-xTa alloys fabricated using the levitation fusion technique was studied in terms of color change, the mass of oxide layer and mechanical properties. The results were compared and they lead to the following conclusions:

- Varying the potential, different colors might be obtained on the surface of the samples; by applying a potential of 100 V, the oxide layer turned to dark gray indicating that the layer is thick enough and the sample does not reflect the light anymore;
- The mass of the oxide layer increased by increasing the passivation voltage, thus at a potential of 100 V the mass of oxide was the highest;
- The hardness values increases with the increase of applied load for each composition which was found to be typical for low testing loads;
- Using a potential of 70 V a reddish oxide color was obtained which might have optimal applications in dentistry because of their aesthetic and mechanical characteristics;
- Among the tested samples, the Ti–25Ta composition proved to have the highest hardness value indicating that an increase of the β phase and the grain refinement does not necessarily improve the mechanical characteristics of the alloy as in the case of Ti–30Ta;
- The Ti–25Ta composition presents the lowest indentation depth indicating that on its surface the oxide layer is more compact compared to the other tested samples.

CRediT authorship contribution statement

Iosif Hulka: Conceptualization, Methodology, Investigation, Writing – original draft. **Nestor R. Florido-Suarez:** Software, Validation, Investigation, Writing – review & editing. **Julia C. Mirza-Rosca:** Conceptualization, Validation, Investigation, Writing – review & editing. **Adriana Saceleanu:** Formal analysis, Resources, Visualization, Supervision.

Declaration of competing interest

The authors declare that they have no known competing financial interests or personal relationships that could have appeared to influence the work reported in this paper.

Acknowledgments

The research was supported by Gran Canaria Cabildo, project number CABINFR2019-07 and the Spanish Ministry of Universities and European Union Maria Zambrano, project number SI-1821.

References

[1] D. Gheorghe, D. Pop, R. Ciocoiu, O. Trante, C. Milea, A. Mohan, H. Benea, V. Saceleanu, Microstructure development in titanium and its alloys used for medical applications, UPB Sci. Bull. Ser. B Chem. Mater. Sci. 81 (2019) 244–258.
[2] Q. Chen, G.A. Thouas, Metallic implant biomaterials, Mater. Sci. Eng. R 87 (2015) 1–57, https://doi.org/10.1016/j.mser.2014.10.001.
[3] P.P. Perdomo-Socorro, N.R. Florido-Suárez, A. Verdú-Vázquez, J.C. Mirza-Rosca, Comparative EIS study of titanium-based materials in high corrosive environments, Int. J. Surf. Sci. Eng. 15 (2021) 152–164, https://doi.org/10.1504/IJSURFSE.2021.116333.

[4] B.Q. Li, R.Z. Xie, X. Lu, Microstructure, mechanical property and corrosion behavior of porous Ti–Ta–Nb–Zr, Bioact. Mater. 5 (2020) 564–568, https://doi.org/10.1016/j.bioactmat.2020.04.014.
[5] S. Rao, T. Ushida, T. Tateishi, Y. Okazaki, S. Asao, Effect of Ti, Al, and V ions on the relative growth rate of fibroblasts (L929) and osteoblasts (MC3T3-E1) cells, Bio Med. Mater. Eng. 6 (1996) 79–86.
[6] I. Cvijović-Alagić, S. Laketić, J. Bajat, A. Hohenwarter, M. Rakin, Grain refinement effect on the Ti-45Nb alloy electrochemical behavior in simulated physiological solution, Surf. Coating. Technol. 423 (2021) 1–9, https://doi.org/10.1016/j.surfcoat.2021.127609.
[7] B.L. Bayode, M.L. Lethabane, P.A. Olubambi, I. Sigalas, M.B. Shongwe, M. M. Ramakokovhu, Densification and micro-structural characteristics of spark plasma sintered Ti-Zr-Ta powders, Powder Technol. 321 (2017) 471–478, https://doi.org/10.1016/j.powtec.2017.08.031.
[8] D. Mareci, R. Chelariu, D.M. Gordin, G. Ungureanu, T. Gloriant, Comparative corrosion study of Ti-Ta alloys for dental applications, Acta Biomater. 5 (2009) 3625–3639, https://doi.org/10.1016/j.actbio.2009.05.037.
[9] P.P. Socorro-Perdomo, N.R. Florido-Suárez, J.C. Mirza-Rosca, M.V. Saceleanu, EIS characterization of Ti alloys in relation to alloying additions of Ta, Materials 15 (2022), https://doi.org/10.3390/ma15020476.
[10] K.A. De Souza, A. Robin, Preparation and characterization of Ti-Ta alloys for application in corrosive media, Mater. Lett. 57 (2003) 3010–3016, https://doi.org/10.1016/S0167-577X(02)01422-2.
[11] E. Hamzah, Z.Z. Anuar, I.S. Arudi, M.K. Ibrahim, A. Bahador, A. Khaatak, Influence of fabrication methods on the microstructures and hardness of Ti-Ni, Ti-Nb and Ti-Ta for biomedical applications, Mater. Today Proc. 39 (2019) 975–978, https://doi.org/10.1016/j.matpr.2020.04.520.
[12] M.A. Tito Patricio, C.J.R. Lustosa, J.A.M. Chaves, P.W.B. Marques, P.S. Silva, A. Almeida, R. Vilar, O. Florêncio, Relationship between microstructure, phase transformation, and mechanical behavior in Ti–40Ta alloys for biomedical applications, J. Mater. Res. Technol. 14 (2021) 210–219, https://doi.org/10.1016/j.jmrt.2021.06.038.
[13] P. Socorro-Perdomo, N. Florido-Suarez, I. Voiculescu, J. Mirza-Rosca, Biocompatibility of new high-entropy alloys with non-cytotoxic elements, Microsc. Microanal. 27 (2021) 1772–1774, https://doi.org/10.1017/s1431927621006486.
[14] W. Plieth, 9 - oxides and semiconductors, in: W. Plieth (Ed.), Electrochemistry for Materials Science, Elsevier, Amsterdam, 2008, ISBN 978-0-444-52792-9, pp. 263–290.
[15] T. Wang, L. Wang, Q. Lu, Z. Fan, Changes in the esthetic, physical, and biological properties of a titanium alloy abutment treated by anodic oxidation, J. Prosthet. Dent 121 (2019) 156–165, https://doi.org/10.1016/j.prosdent.2018.03.024.
[16] R. Cosgarea, C. Gasparik, D. Dudea, B. Culic, B. Dannewitz, A. Sculean, Peri-implant soft tissue colour around titanium and zirconia abutments: a prospective randomized controlled clinical study, Clin. Oral Implants Res. 26 (2015) 537–544, https://doi.org/10.1111/clr.12440.
[17] E. Bressan, G. Paniz, D. Lops, B. Corazza, E. Romeo, G. Favero, Influence of abutment material on the gingival color of implant-supported all-ceramic restorations: a prospective multicenter study, Clin. Oral Implants Res. 22 (2011) 631–637, https://doi.org/10.1111/j.1600-0501.2010.02008.x.
[18] T. Linkevicius, J. Vaitelis, The effect of zirconia or titanium as abutment material on soft peri-implant tissues: a systematic review and meta-analysis, Clin. Oral Implants Res. 26 (2015) 139–147, https://doi.org/10.1111/clr.12631.
[19] R. Charrière, G. Lacaille, M.P. Pedeferri, J. Faucheu, D. Delafosse, Characterization of the gonioapparent character of colored anodized titanium surfaces, Color Res. Appl. 40 (2015) 483–490, https://doi.org/10.1002/col.21911.
[20] J. Chávez, O. Jimenez, J. Diaz-Luna, D. Bravo-Barcenas, F. Alvarado-Hernández, M. Flores, R. Suárez-Martínez, Microstructure and corrosion characterization of a Ti-30Zr alloy with Ta additions processed by arc-melting for biomedical applications, Mater. Lett. 284 (2021), 129041, https://doi.org/10.1016/j.matlet.2020.129041.
[21] A. Karambakhsh, A. Afshar, S. Ghahramani, P. Malekinejad, Pure commercial titanium color anodizing and corrosion resistance, J. Mater. Eng. Perform. 20 (2011) 1690–1696, https://doi.org/10.1007/s11665-011-9860-0.
[22] J.-L. Delplancke, M. Degrez, A. Fontana, R. Winand, Self-colour anodizing of titanium, Surf. Technol. 16 (1982) 153–162.
[23] S. Van Gils, P. Mast, E. Stijns, H. Terryn, Colour properties of barrier anodic oxide films on aluminium and titanium studied with total reflectance and spectroscopic ellipsometry, Surf. Coating. Technol. 185 (2004) 303–310, https://doi.org/10.1016/j.surfcoat.2004.01.021.
[24] M. Pourbaix, H. Zhang, A. Pourbaix, Presentation of an Atlas of chemical and electrochemical equilibria in the presence of a gaseous phase, Mater. Sci. Forum 251–254 (1997) 143–148. https://doi.org/10.4028/www.scientific.net/msf.251-254.143.
[25] N.K. Kuromoto, R.A. Simão, G.A. Soares, Titanium oxide films produced on commercially pure titanium by anodic oxidation with different voltages, Mater. Char. 58 (2007) 114–121, https://doi.org/10.1016/j.matchar.2006.03.020.
[26] M.V. Diamanti, B. del Curto, M. Pedeferri, Anodic oxidation of titanium: from technical aspects to biomedical applications, J. Appl. Biomater. Biomech. 9 (2011) 55–69, https://doi.org/10.5301/JABB.2011.7429.
[27] S. Dayarambhai Kahar, A. Singh, S. Kahar, V. Patel, U. Kanetkar, U.G. Student, Anodizing of Ti and Ti alloys for different applications: a review "corrosion behaviour and colour properties of anodized titanium" view project anodizing of Ti and Ti alloys for different applications: a review, IJSRD-International J. Sci. Res. Dev. 8 (2020), 2321–0613.
[28] N. Ibriş, J.C. Mirza Rosca, EIS study of Ti and its alloys in biological media, J. Electroanal. Chem. 526 (2002), https://doi.org/10.1016/S0022-0728(02)00814-8.
[29] J.E.G. González, J.C. Mirza-Rosca, Study of the corrosion behavior of titanium and some of its alloys for biomedical and dental implant applications, J. Electroanal. Chem. 471 (1999) 109–115, https://doi.org/10.1016/S0022-0728(99)00260-0.
[30] A.I. Mardare, A. Savan, A. Ludwig, A.D. Wieck, A.W. Hassel, A combinatorial passivation study of Ta-Ti alloys, Corrosion Sci. 51 (2009) 1519–1527, https://doi.org/10.1016/j.corsci.2008.12.003.
[31] P. Marcus, On some fundamental factors in the effect of alloying elements on passivation of alloys, Corrosion Sci. 36 (1994) 2155–2158, https://doi.org/10.1016/0010-938X(94)90013-2.
[32] M. Janik-Czachor, A. Jaskiewicz, P. Kedzierzawski, Z. Werner, Stability of the passive state of Al–Ta and Al–Nb amorphous alloys, Mater. Sci. Eng. 358 (2003) 171–177, https://doi.org/10.1016/S0921-5093(03)00332-0.
[33] M. Lewandowska, M. Pisarek, K. Rożniatowski, M. Grądzka-Dahlke, M. Janik-Czachor, K.J. Kurzydłowski, Nanoscale characterization of anodic oxide films on Ti-6Al-4V alloy, Thin Solid Films 515 (2007) 6460–6464, https://doi.org/10.1016/j.tsf.2006.11.074.
[34] K. Sangwal, B. Surowska, P. Blaziak, Analysis of the indentation size effect in the microhardness measurement of some cobalt-based alloys, Mater. Chem. Phys. 77 (2003) 511–520, https://doi.org/10.1016/S0254-0584(02)00086-X.
[35] J. Petrík, P. Palfy, The influence of the load on the hardness, Metrol. Meas. Syst. 18 (2011) 5, https://doi.org/10.2478/v10178-011-0005-5.
[36] D. Zhao, C. Han, Y. Li, J. Li, K. Zhou, Q. Wei, J. Liu, Y. Shi, Improvement on mechanical properties and corrosion resistance of titanium-tantalum alloys in-situ fabricated via selective laser melting, J. Alloys Compd. 804 (2019) 288–298, https://doi.org/10.1016/j.jallcom.2019.06.307.
[37] Y. Liu, K. Li, H. Wu, M. Song, W. Wang, N. Li, H. Tang, Synthesis of Ti-Ta alloys with dual structure by incomplete diffusion between elemental powders, J. Mech. Behav. Biomed. Mater. 51 (2015) 302–312, https://doi.org/10.1016/j.jmbbm.2015.07.004.
[38] R.R. Boyer, G. Welsch, E.W. Collings, Materials Properties Handbook: Titanium Alloys, 1994.
[39] Florido-Suarez, Nestor, Verdu-Vazquez, Amparo, Socorro-Perdomo, Pedro, J. C. Mirza-Rosca, Past advances and future perspective of Ti-Ta alloys, Glob. J. Eng. Sci. 7 (2021) 20–22, https://doi.org/10.33552/gjes.2021.07.000668.